

Characterization of classical Gaussian processes using quantum probes

Claudia Benedetti, Matteo G. A. Paris

Dipartimento di Fisica, Università degli Studi di Milano, I-20133 Milano, Italy

Abstract

We address the use of a single qubit as a quantum probe to characterize the properties of classical noise. In particular, we focus on the characterization of classical noise arising from the interaction with a stochastic field described by Gaussian processes. The tools of quantum estimation theory allow us to find the optimal *state preparation* for the probe, the optimal *interaction time* with the external noise, and the optimal *measurement* to effectively extract information on the noise parameter. We also perform a set of simulated experiments to assess the performances of maximum likelihood estimator, showing that the asymptotic regime, where the estimator is unbiased and efficient, is approximately achieved after few thousands repeated measurements on the probe system.

1. Introduction

Quantum systems of interest for quantum technology are usually immersed in complex environments, which influence their dynamics and generally induce decoherence. The characterization of the environment properties is thus a relevant topic for the development of effective quantum protocols. In many situations, the environment may be conveniently represented as a collection of fluctuators, such that it can be described as a classical stochastic field, e.g. driven by a Gaussian process. In fact, much attention has been recently devoted to answering the question whether even a quantum bath can be described using a classical or semi-classical picture of the environment [1, 2, 3, 4, 5]. The classical description becomes progressively more reliable as far as the environment has many degrees of freedom or when the interaction between a quantum system and a classical fluctuating field is taken into account. Several systems of interest indeed belong to this category, including the dynamics of quantum correlations in the presence of classical fluctuations [6, 7, 8, 9, 10], the simulation of motional averaging [11], and the decoherence problem associated to the non-Markovian dynamics of solid state qubits [12, 13, 14].

A reliable characterization of the environment, e.g. through its power spectrum, may allow one to design robust quantum protocols resilient to noise [15, 16, 17, 18]. To this aim, some efforts have been recently devoted to understand whether the (de)coherent dynamics of a qubit can be used to extract information on the noise affecting the qubit itself [19, 20, 21, 22]. The canonical way to attack this problem is by using the tools of quantum estimation theory (QET) [23, 24, 25, 26, 27, 28]. Indeed, QET allows one to individuate the best strategy to estimate the value of an unknown parameter, even when it corresponds to a quantity which is not accessible by direct measurement. Upon collecting the outcomes from the measurement of a suitably optimized observable, it is possible to build an estimator and infer the value of the parameter with the ultimate precision allowed by quantum mechanics. QET has

been effectively employed in several scenarios, e.g to estimate quantum correlations [29, 30], interferometric phase-shift [31, 32, 33, 34, 35, 36, 37, 38, 39], and the spectral properties of non-Gaussian environments [20, 21]. Concerning quantum probes, optimized quantum thermometry by single qubit has been recently addressed experimentally [40, 41] and theoretically [42, 43].

In this paper we address the characterization of classical noise using a qubit as a quantum probe, and focus attention to noise generated by Gaussian stochastic processes, i.e. processes that are fully described by their power spectrum or their autocorrelation function. A relevant example of Gaussian process is the Ornstein-Uhlenbeck process, which has been extensively employed in various contexts [44, 45, 46, 47]. For the sake of completeness, and in order to analyze possible effects due to specific features of the noise spectra, we also consider the noise generated by processes with a Gaussian or a power law autocorrelation function.

The performances of a qubit as a quantum probe clearly depend on the kind of interaction it establishes with the environment. In order to maintain the analysis self-contained, and to address situations of practical interest, in the following we will assume that the dephasing effects of the environment are much stronger than relaxation (damping) ones. This generally happens when the typical frequencies of the environment are smaller than the natural frequencies of the system, i.e. the energy splitting between the eigenstates of the unperturbed Hamiltonian. In this case, in fact, fluctuations can cause a superposition to decohere, without driving transitions between the different levels. In this framework, the characterization of the noise, which consists in estimating the parameters of the autocorrelation function, amounts to estimate the characteristic time describing the dephasing process occurring during the decoherent dynamics.

Due to the relatively simple dynamics of the probe, we have been able to evaluate the quantum Fisher information (QFI) and the quantum signal-to-noise ratio (QSNR) analytically. Upon

maximizing the QFI we obtain the three ingredients required to build an optimized inference strategy to characterize the noise, i.e.: i) the optimal initial state preparation for the qubit; ii) the optimal interaction time with the environment; iii) the optimal measurement to be performed at the output. The final step is then the processing of data to infer the value of the noise parameter, for which we employ a maximum likelihood estimator (MLE). In order to assess the performances of MLE we have performed a set of simulated experiments, showing that the asymptotic regime, where it becomes unbiased and efficient, is approximately achieved after few thousands repeated measurements on the probe system.

The paper is organized as follows: in Sec. 2 we introduce the physical model for the qubit-environment system and describe the Gaussian processes generating the noise; in Sec. 3 we briefly review the tools of local quantum estimation theory; in Sec. 4 we present our results about the optimal settings to achieve a large QFI and the performances of a likelihood estimator. In Sec. 5 we end the paper with some concluding remarks.

2. The physical model

Consider a qubit interacting with a classical fluctuating field which induces dephasing. The qubit Hamiltonian is given by

$$\mathcal{H}(t) = \omega_0 \sigma_z + B(t) \sigma_z, \quad (1)$$

where ω_0 is the qubit energy, σ_z is the Pauli matrix, and $B(t)$ is a stochastic stationary process that follows a Gaussian statistics. In particular, we focus on processes characterized by a zero mean and a autocorrelation function $K(t, t')$, in formula:

$$[B(t)]_B = 0 \quad (2)$$

$$[B(t)B(t')]_B = K(t - t') \quad (3)$$

where $[...]_B$ represents the average over the stochastic process B . A Gaussian process is fully described by its second order statistics, e.g. its autocorrelation function K . The characteristic function is given by [48, 49]:

$$\left[e^{i \int_0^t ds f(s) B(s)} \right]_B = e^{-\frac{1}{2} \int_0^t ds \int_0^t ds' f(s) K(s-s') f(s')}. \quad (4)$$

From the Hamiltonian (1), we can write the time evolution operator

$$U(t) = \exp \left\{ -i \int_0^t \mathcal{H}(s) ds \right\} = \exp \{ -i [\omega_0 t + \varphi(t)] \sigma_z \}, \quad (5)$$

where we defined the noise phase $\varphi(t) = \int_0^t B(s) ds$. We assume that the qubit is initially in a pure state $|\psi_0\rangle = \cos \theta/2 |0\rangle + \sin \theta/2 |1\rangle$ with $0 < \theta < \pi$. The qubit density matrix is given by the average of the evolved density matrix over the stochastic process:

$$\rho(t) = [U(t) \rho(0) U^\dagger(t)]_B = \frac{1}{2} \begin{pmatrix} 1 + \cos \theta & e^{-2i\omega_0 t} [e^{-2i\varphi(t)}]_B \sin \theta \\ e^{2i\omega_0 t} [e^{2i\varphi(t)}]_B \sin \theta & 1 - \cos \theta \end{pmatrix}, \quad (6)$$

where the initial state is $\rho(0) = |\psi_0\rangle\langle\psi_0|$. We can rewrite Eq. (6) as:

$$\rho(t) = \frac{1}{2} \begin{pmatrix} 1 + \cos \theta & e^{-2(i\omega_0 t + \beta(t))} \sin \theta \\ e^{2(i\omega_0 t - \beta(t))} \sin \theta & 1 - \cos \theta \end{pmatrix}, \quad (7)$$

where the off diagonal terms are calculated using Eq. (4) and the function β is related to the autocorrelation function of the stochastic process generating the classical noise through the relation:

$$\beta(t) = \int_0^t \int_0^t ds ds' K(s - s'). \quad (8)$$

In this paper we consider three particular Gaussian processes. Specifically, we assume that the stochastic field $B(t)$ in Eq. (1) is driven either by an Ornstein-Uhlenbeck (OU), or by a Gaussian (G) or power-law (PL) one. The corresponding autocorrelation functions are given by

$$K_{OU}(t - t', \gamma, \Gamma) = \frac{\Gamma \gamma}{2} e^{-\gamma|t-t'|} \quad (9)$$

$$K_G(t - t', \gamma, \Gamma) = \frac{\Gamma \gamma}{\sqrt{\pi}} e^{-\gamma^2(t-t')^2} \quad (10)$$

$$K_{PL}(t - t', \gamma, \Gamma, \alpha) = \frac{\alpha - 1}{2} \frac{\gamma \Gamma}{(\gamma|t - t'| + 1)^\alpha} \quad (11)$$

where γ is the unknown noise parameter, Γ is the damping rate that we assume fixed, and t is the interaction time. In Eq. (11) we have the constraint $\alpha > 2$. Inserting these autocorrelation functions in Eq. (8) leads to the following β functions:

$$\beta_{OU}(g, \tau) = \frac{1}{g} (g\tau + e^{-g\tau} - 1) \quad (12)$$

$$\beta_G(g, \tau) = \frac{1}{g} \left[g\tau \operatorname{Erf}(g\tau) + \frac{e^{-(g\tau)^2} - 1}{\sqrt{\pi}} \right] \quad (13)$$

$$\beta_{PL}(g, \tau) = \frac{1}{g} \left[\frac{(1 + g\tau)^{2-\alpha} + g\tau(\alpha - 2) - 1}{(\alpha - 2)} \right]. \quad (14)$$

where we introduced the adimensional quantities $g = \frac{\gamma}{\Gamma}$ and $\tau = \Gamma t$.

The characterization of the classical noise amounts to estimate the overall noise parameter g by performing measurements on the quantum probe after the interaction, i.e. on the states described by the density matrices in Eq. (7). In order to make this procedure as effective as possible, i.e. to extract the maximum amount of information on the noise by inspecting the state of the probe, we have to suitably optimize the initial preparation of the qubit, the value of the interaction time, the measurement to be performed at the output and, finally, the data processing after collecting an experimental sample. The proper framework to attack this optimization problem is that of local quantum estimation theory [23, 24, 25, 26, 27, 28], which we are going to briefly review in the next Section.

3. Quantum estimation theory

Consider a family of quantum states ρ_γ , characterized by an unknown value of a parameter γ , usually corresponding to a

non-observable quantity. The goal of any estimation procedure is to infer the value of the unknown parameter γ by measuring some observable quantity on the system ρ_γ . This is achieved by collecting the outputs (x_1, x_2, \dots, x_M) of such measurements and use them to build an estimator $\hat{\gamma} = \hat{\gamma}(x_1, x_2, \dots, x_M)$, i.e. a function of the outcomes. The smaller is the estimator variance σ^2 (over data), the more accurate is the estimation procedure. The lower bound to the precision of any unbiased estimator is given by the Cramér-Rao (CR) bound:

$$\sigma^2(\hat{\gamma}) \geq \frac{1}{MF(\gamma)}, \quad (15)$$

where M is the number of measurements and $F(\gamma)$ is the Fisher Information (FI):

$$F(\gamma) = \sum_x p(x|\gamma) \left[\partial_\gamma \ln p(x|\gamma) \right]^2, \quad (16)$$

where $p(x|\gamma)$ is the conditional probability of obtaining the outcomes x if the true value of the parameter is γ . Given a quantum system, the conditional probability can be written as $p(x|\gamma) = \text{Tr}[\rho_\gamma E_x]$ with E_x a positive operator-valued measure (POVM). By maximizing the FI over all possible POVMs (see e.g. [27]), one obtains the ultimate bound to the precision of any estimator, i.e. the quantum Cramer-Rao (QCR) bound:

$$\sigma^2(\hat{\gamma}) \geq \frac{1}{MH(\gamma)}, \quad (17)$$

where $H(\gamma)$ is the quantum Fisher information, i.e. the superior of $F(\gamma)$ over POVMs. A measurement E_x is said to be *optimal* when its FI coincides with the QFI, i.e. $F(\gamma) = H(\gamma)$. Eqs. (15) and (17) set the lower bound to the precision of any estimation procedure. Once a measurement has been chosen, and performed, one has to process data, i.e. to choose an estimator. Estimators for which the CR bound is saturated are said to be *efficient*.

For a family of qubit states, the QFI reads:

$$H(\gamma) = \sum_{n=1}^2 \frac{(\partial_\gamma p_n)^2}{p_n} + 2 \sum_{n \neq m} \frac{(p_n - p_m)^2}{p_n + p_m} |\langle p_m | \partial_\gamma p_n \rangle|^2 \quad (18)$$

where p_n and $|p_n\rangle$ are respectively the eigenvalues and eigenvectors of the qubit density matrix $\rho = \sum_{n=1,2} p_n |p_n\rangle\langle p_n|$.

A suitable figure of merit to assess the overall estimability of a parameter is the quantum signal-to-noise ratio (QSNR):

$$R(\gamma) = \gamma^2 H(\gamma), \quad (19)$$

which accounts for the fact that large values of the parameter are generally easier to estimate, while small values need more precise estimators. A given parameter is said to be easily estimable if the corresponding R is large. On the other hand, if R is small the estimation of γ is an inherently inefficient procedure, whatever strategy is employed to infer its value.

Once a measurement has been chosen, possibly the optimal one maximizing the Fisher information, one has to chose an estimator, i.e. a procedure to process data in order to infer the

value of the parameter of interest. An estimator which is *asymptotically efficient*, i.e. it saturates the QCR bound in the limit of large samples, is the maximum likelihood estimator. Consider M independent measurements of the random variables X , with probability density $p(x|\gamma)$. The joint probability function of an experimental sample of size M , $\{x_i\}_{i=1}^M$, is given by the product $\prod p(x_i, \gamma)$, and it is usually referred to as the Likelihood function $L(\gamma)$

$$L(\gamma) = L(\gamma|x_1, x_2, \dots, x_M) = \prod_{i=1}^M p(x_i|\gamma). \quad (20)$$

The MLE for the parameter γ is the value yielding the largest likelihood of the observed values, that is the value that maximizes the quantity in Eq. (20):

$$\hat{\gamma}_{ML} = \arg \max_{\gamma} L(\gamma). \quad (21)$$

As mentioned above, γ_{ML} is known to be asymptotically efficient [50], i.e. it saturates the CR bound for large number of measurements $M \gg 1$. On the other hand, in practical situations, one is usually interested in checking whether this regime is achieved for values of M within the experimental capabilities.

4. Quantum probes for classical environments

In this section we present and discuss our results. In the first subsection, we find the analytic expressions of the QFI and the QSNR for the estimation of the noise parameter g of the considered processes. Moreover, we show that the optimal measurement corresponds to the Pauli matrix σ_x in the rotating frame of the qubit. In the second subsection we assess the performances of the MLE by a set of simulated experiments.

4.1. Signal-to-noise ratio and optimal setting

The QFI gives the ultimate quantum bound to the precision of an inference procedure. For the family of qubit density matrices described by Eq. (7), the QFI can be computed using Eq. (18), through the eigenvalues and eigenvectors of the density operator:

$$p_{\pm}(g, \tau) = \frac{1}{2} \left(1 \pm e^{-2\beta(g, \tau)} \right) \quad (22)$$

$$|p_{\pm}\rangle = \frac{1}{\sqrt{2}} \left(\pm e^{-2i\omega_0 \tau} |0\rangle + |1\rangle \right). \quad (23)$$

where we substituted the symbol $p_{1,2}$ with p_{\pm} to denote eigenvalues and eigenvectors. Inserting these expressions in Eq. (18), one obtains the analytic expression for the QFI:

$$H(g, \tau) = 4 \frac{\sin^2 \theta}{e^{4\beta(g, \tau)} - 1} \left[\partial_g \beta(g, \tau) \right]^2. \quad (24)$$

It is worth noticing that Eq. (24) does not depend on the qubit energy ω_0 , and it is maximized by $\theta = \frac{\pi}{2}$. It follows that the optimal initial state is the superposition $|\psi_0\rangle = \frac{1}{\sqrt{2}}(|0\rangle + |1\rangle) = |+\rangle$.

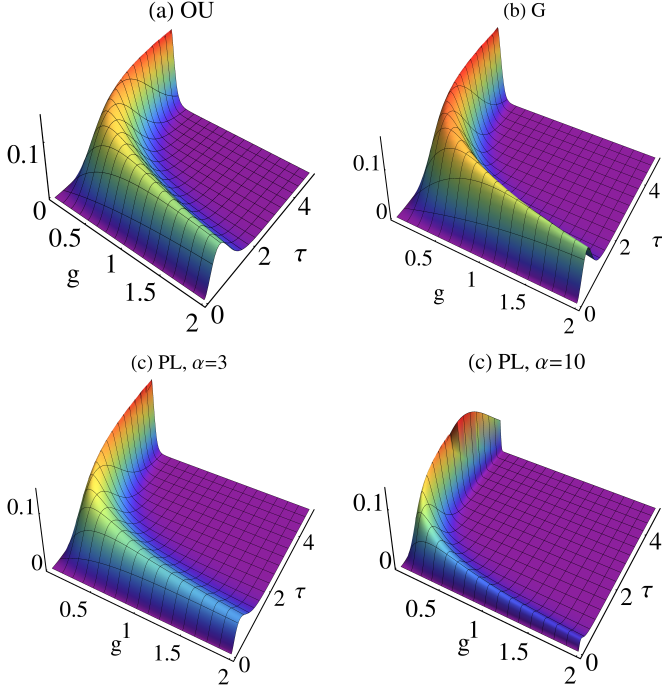


Figure 1: (Color online): The quantum signal-to-noise ratio $R(g)$ as a function of g and the interaction time τ for different stochastic processes: (a) OU, (b) G, and PL with (c) $\alpha = 3$ and (d) $\alpha = 10$.

For the processes described in Eqs. (12)-(14), the QSNR is calculated from Eq. (19) and it is given by:

$$\begin{aligned}
 R_{OU}(g, \tau) &= \frac{4e^{-2g\tau}}{g^2} \left[\frac{(1 - e^{g\tau} + g\tau)^2}{e^{4(\tau + \frac{e^{-g\tau}-1}{g})} - 1} \right] \\
 R_G(g, \tau) &= \frac{4}{\pi g^2} \left[\frac{(e^{-g^2\tau^2} - 1)^2}{e^{4(\frac{e^{-g^2\tau^2}-1}{\sqrt{\pi}g} + \tau \text{Erf}(g\tau))} - 1} \right] \\
 R_{PL}(g, \tau) &= \frac{4}{g^2} \left[\frac{(1 + \alpha g\tau + (\alpha - 1)(g\tau)^2 - (1 + g\tau)^\alpha)^2}{\left(e^{4\left(\tau + \frac{(1+g\tau)^{2-\alpha}-1}{g(\alpha-2)}\right)} - 1 \right) (\alpha - 2)^2 (1 + g\tau)^{2\alpha}} \right]
 \end{aligned} \quad (25)$$

The QSNRs of Eqs. (25) are shown in Fig. 1. As it is apparent from the plots, the qualitative behavior is the same for all processes. At any fixed value of g there is a maximum in the QSNR, achieved for an optimal value of the interaction time $\tau_M(g)$. The value of this maximum $R_M = R(\tau_M)$ decreases with g . It follows that smaller values of g may be better estimated than larger ones. The optimal time $\tau_M(g)$ decreases with increasing values of the parameter. This means that the smaller is g , the longer is the interaction time that is required to effectively imprint the effects of the external environment on the probe. The dependency of τ_M on the parameter g is shown in the upper panel of Fig. 2, for the three considered processes. For small values of g we have approximately $\tau_M \simeq a/\sqrt{g}$ (with $a \simeq 0.89$ for OU and similar values for the other processes) while for $g \gg 1$ we may write $\tau_M \simeq b/g$, with $b \simeq 2.5$ for OU.

The corresponding values of the QSNR, i.e. R_M are shown in the lower panel of the same figure. R_M is almost constant for small g and then start to decrease. We have $R_M \simeq a - b\sqrt{g}$ for $g \ll 1$, where $a \simeq 0.161$ and $b = 0.096$ for OU, and $R_M \simeq b/g$ for $g \gg 1$, with $b \simeq 0.33$ for OU. It follows that g may be effectively estimated when it is small, since the QSNR is large. In this regime, the estimation procedure is also robust, since the optimal interaction time and the resulting value of the QSNR depend only weakly on the value of g . On the other hand, for larger g the estimation procedure is unavoidably less effective.

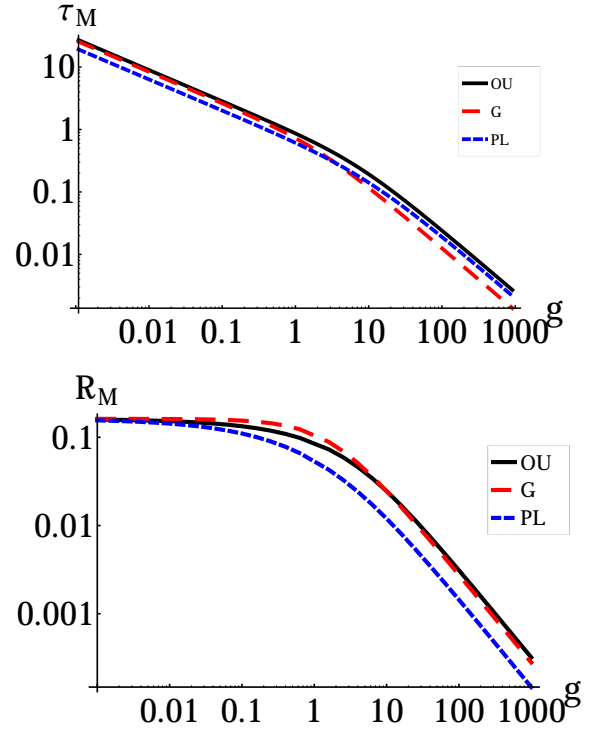


Figure 2: (Color online): The upper panel shows the optimal interaction time $\tau_M(g)$, which maximizes the QSNR, for the three different processes. We have OU (solid black), G (dashed red) and PL (dotted blue). In the PL case, we set $\alpha = 3$. The lower panel shows the corresponding (maximized) values of the QSNR R_M , using the same color code.

To complete our analysis, we now prove that the optimal measurement achieving the QFI is a realistic one, since it corresponds to the projectors onto the eigenstates (23). In fact, the FI of the distributions (22), computed from Eq. (16), is given by:

$$\begin{aligned}
 F(g, \tau) &= \frac{[\partial_g p_+(g, \tau)]^2}{p_+(g, \tau)} + \frac{[\partial_g p_-(g, \tau)]^2}{p_-(g, \tau)} \\
 &= \frac{4 [\partial_g \beta(g, \tau, t)]^2}{e^{4\beta(g, \tau)} - 1} = H(g, \tau),
 \end{aligned} \quad (26)$$

which coincides with the QFI. The optimal measurement is thus obtained from the projectors onto the eigenstates of the density

matrix $\Pi_{\pm} = |p_{\pm}\rangle\langle p_{\pm}|$:

$$\Pi_{\pm} = \frac{1}{2} \begin{pmatrix} 1 & \pm e^{-2i\omega_0 t} \\ \pm e^{2i\omega_0 t} & 1 \end{pmatrix} \quad (27)$$

$$= \frac{1}{2} e^{-i\omega_0 t \sigma_z} |\pm\rangle\langle\pm| e^{i\omega_0 t \sigma_z}. \quad (28)$$

In other words, the optimal measurement corresponds to σ_x in the qubit reference frame which rotates with frequency ω_0 .

4.2. Maximum Likelihood estimator

In this Section we present the results of simulated experiments, performed to assess the performances of the MLE and to characterize its asymptotic regime. In particular, we have numerically simulated repeated measurements of the observable described by the projectors Π_{\pm} in Eq. (28), and then estimated the value of the parameter g in the case of OU process using MLE.

Let us consider to have performed M repeated measurements of Π_{\pm} at the optimal time τ_M . Each run returns ± 1 , according to the probability distributions (22). Let us call N the number of outcomes with value $+1$. The frequentist interpretation of probability leads us to write the relation

$$p_+(g, \tau) = \frac{N}{M}, \quad (29)$$

implicitly assuming that the number of measurement is large $M \gg 1$.

In order to simplify the notation, we hereafter call $p(g, \tau) \equiv p_+(g, \tau)$. By inverting Eq. (29), we can write the inversion estimator \hat{g} of g : $\hat{g}(N, M) = p^{-1}\left(\frac{N}{M}, \tau\right)$. Before analyzing the performances of this estimator we show that it coincides with the MLE. In fact, from Eqs. (20) and (21) we have:

$$P_L(g, \tau) = p(g, \tau)^N [1 - p(g, \tau)]^{M-N} \quad (30)$$

$$\partial_g P_L(g, \tau) = -[1 - p(g, \tau)]^{M-N-1} p(g, \tau)^{N-1} \times [Mp(g, \tau) - N] \partial_g p(g, \tau). \quad (31)$$

Eq. (31) has a maximum for $p(g, \tau) = \frac{N}{M}$ which, by inversion, gives the inversion estimator

$$\hat{g}_{ML}(N, M) = p^{-1}\left(\frac{N}{M}, \tau\right). \quad (32)$$

The MLE is a function of the number of repeated measurements M and the number of outcomes with value $+1$, N . By numerical simulations, we mimic the results of experiments. The variance of the MLE (32) is computed using the error propagation theory. Upon assuming that the measure outcomes follow a binomial distribution, the estimator variance σ^2 is given by:

$$\sigma^2(\hat{g}_{ML}) = \left| \frac{\partial \hat{g}_{ML}(N, M)}{\partial N} \right|^2 N \left(1 - \frac{N}{M}\right). \quad (33)$$

In Fig. 3 we show the ratio between the estimated value \hat{g}_{ML} and the true value as a function of the number of repeated measurements for different values of the true parameter g . The estimated value oscillates around the true one, with standard deviations σ decreasing as a function of M . In fact, as the number

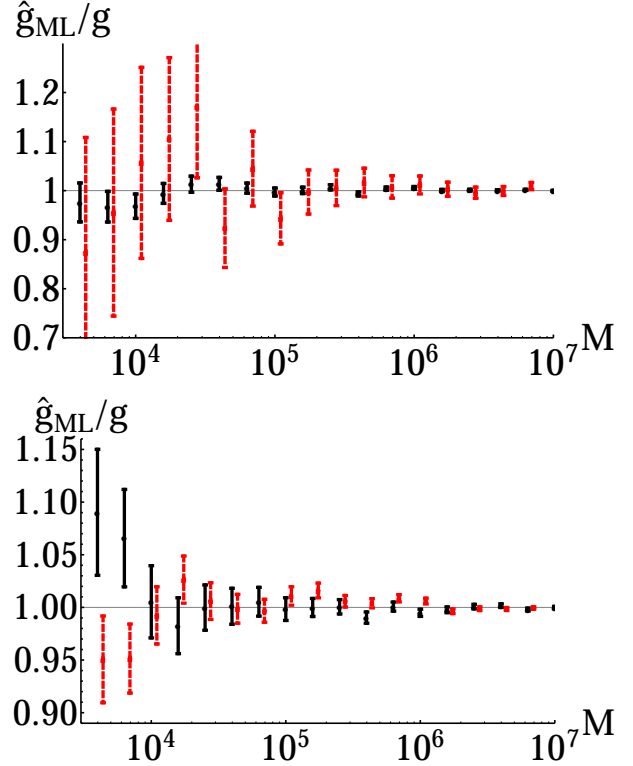


Figure 3: (Color online): The two panels show the ratio g_{ML}/g between the ML estimated value of g and the true value, together with the corresponding error bars, as a function of the number of repeated (simulated) measurements M . In the upper panel the results for the true values $g = 0.01$ (solid black) and $g = 100$ (red dashed) are compared. Larger values of the parameter are better estimated. In the lower panel the considered values are $g = 0.1$ (solid black) and $g = 1$ (red dashed). Notice that the simulated data in both panels are computed for the same values of M and then the red points are slightly shifted along the x -axes for the sake of clarity.

of measurements becomes larger, the ratio g_{ML}/g gets closer to unity. The error associated to each point is smaller with increasing number of measurements. The sets of data in Fig. 3 refer to $g = 0.01$ (black solid line) and $g = 100$ (red dashed line) in the upper panel and $g = 0.1$ (black solid line) and $g = 1$ (red dashed line) in the lower one. The upper panel in Fig. 3 highlights the fact that for the data associated to small g , the ratio converges more rapidly to unity and with smaller error with respect to the case $g = 100$. This is in agreement with the results of the previous subsection, where we found that R_M is larger for smaller values of the parameter, meaning that the parameter is better estimable in the regime $g \ll 1$. The lower panel of Fig. (3) confirm the behavior found in Fig. 2: in the region $g < 1$ it is possible to easily estimate the parameter almost independently on the value of g .

As already mentioned, the variance σ^2 decreases with increasing M . This is expected from the QCR bound in Eq. (17) because the QFI is a fixed quantity for fixed g , so the minimum error scales as $\frac{1}{M}$.

In Fig. 4 we illustrate the behavior of the variance σ^2 as a function of the measurement number in the case $g = 1$. The red line represents the variance and the shaded area outlines

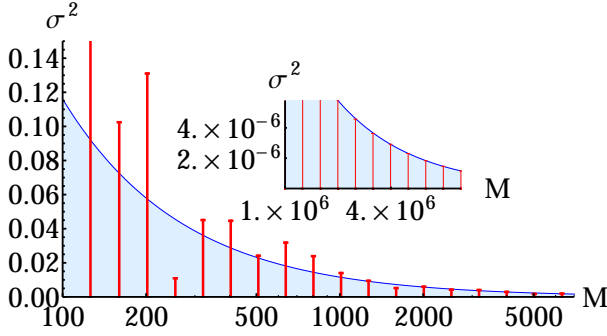


Figure 4: (Color online): The variance (red line) of the ML estimator as a function of the number of measurements for the case $g = 1$. The light blue area illustrates the QCR bound. Variances below the quantum bound mean that the estimator has a bias. Inset: The same as in the main frame but for a large number of measurements: the bias is no longer present.

the QCR bound. The reader may note that in certain cases the variance is below the quantum bound. This means that the estimator is slightly biased. But as the number of measurements is increased the bias tends to zero and the estimator becomes efficient (i.e. it saturates the QCR bound, as shown in the inset) as expected for MLE. The same qualitative behavior is found for all the other values of the parameter g . From our analysis, we see that the asymptotic regime for MLE is already achieved for a number of repeated measurements of about $10^4 - 10^5$. We have also analyzed the convergence of a Bayesian estimator and found that the required M to have the asymptotic behavior is larger. It follows that, to achieve the characterization of the spectral properties of a Gaussian noise, a ML procedure lead to a faster estimation of the unknown parameters.

5. Conclusions

A detailed description of decoherence is crucial for the development of quantum information processing in realistic scenarios. In particular, the precise characterization of the noise acting on a quantum system is the main tool in designing protocols to contrast its detrimental effects. In this paper, we have addressed the estimation of the noise parameter for Gaussian processes by the use a simple quantum system, such as a qubit, as a quantum probe. More specifically, by maximizing the quantum signal-to-noise ratio we have found the optimal setting to perform optimal measurements and inference. Our results show that for any fixed value of the estimable parameter, the QSNR has a maximum, corresponding to an optimal value of the interaction time τ_M . This maximum is larger for smaller values of the parameter, which may be estimated more precisely.

The ultimate bound to precision may be practically achieved by measuring the "polarization" of the qubit, i.e. the observable σ_x in the rotating frame of the qubit, and then employing a maximum-likelihood estimator, which achieves the asymptotic regime, and thus the optimal performances, already after few thousands measurements.

The estimation scheme presented in this paper would be suitable also to infer the amplitude of white noise, characterized by

an autocorrelation function K proportional to a Dirac delta. In this case, the optimal state preparation and measurement are the same as those obtained for Gaussian noise. However, the quantum signal-to-noise-ratio is a monotonically decreasing function of time, leaving no room for any optimization procedure.

At present, we cannot provide a quantitative statement about the performance of quantum probes compared to classical ones since the modelling of the latter would be rather challenging. On the other hand, our results show that quantum probes, besides having the advantage of introducing small perturbations into the system, require only measurements performed at a single instant of time, thus avoiding the need of observing the system for a long time in order to collect a time series.

Acknowledgments

This work has been supported by the MIUR project FIRB-LiCHIS-RBFR10YQ3H. The authors thank the FIM Department of University of Modena and Reggio Emilia for hospitality and an anonymous referee for useful suggestions.

References

References

- [1] I. Neder, M. S. Rudner, H. Bluhm, S. Foletti, B. I. Halperin, A. Yacoby, *Phys. Rev. B*, **84**, 035441 (2011).
- [2] M. J. Biercuck, H. Bluhm, *Phys. Rev. B* **83**, 235316 (2011).
- [3] W. M. Witzel, K. Young and S. Das Sarma, *ArXiv:1307.2597v1*.
- [4] T. Fink, H. Bluhm, *arXiv:1402.0235v1*.
- [5] D. Crow, R. Joynt, *Phys. Rev. A* **89**, 042123 (2014).
- [6] T. Yu, J. H. Eberly, *Opt. Comm.* **283** (2010) 676.
- [7] J.-Q. Li and J.-Q. Liang, *Phys. Lett. A*, **375**, 1496 (2011).
- [8] C. Benedetti, F. Buscemi, P. Bordone, M. G. A. Paris, *Phys. Rev. A* **87**, 052328 (2013).
- [9] C. Benedetti, F. Buscemi, P. Bordone and M. G. A. Paris, *Int. J. Quantum Inform.* **10**, 1241005 (2012).
- [10] i P. Bordone, F. Buscemi and C. Benedetti, *Fluct. Noise Lett.* **11**, 1242003 (2012).
- [11] J. Li, M. P. Silvestri, K. S. Kumar, J.-M. Pirkkalainen, A. Vepsäläinen, W. C. Chien, J. Tuorila, M. A. Sillanpää, P. J. Hakonen, E. V. Thuneberg, and G. S. Paraoanu, *Nat. Commun.* **4**, 1420 (2013).
- [12] G. Bukard, *Phys. Rev. B* **79**, 125317 (2009).
- [13] H. J. Wold, H. Brox, Y. M. Galperin, and J. Bergli *Phys. Rev. B* **86**, 205404 (2012).
- [14] C. Benedetti, M. G. A. Paris, and S. Maniscalco, *Phys. Rev. A* **89**, 012114 (2014).
- [15] J. Bylander, S. Gustavsson, F. Yan, F. Yoshihara, K. Harrabi, G. Fitch, D. G. Cory, Y. Nakamura, J.-S. Tsai, W. D. Oliver, *Nat. Phys.* **7**, 565 (2011).
- [16] J. Zhang, X. Peng, N. Rajendran, and D. Suter, *Phys. Rev. A* **75**, 042314 (2007).
- [17] M. A. A. Ahmed, G. A. Álvarez, D. Suter, *Phys. Rev. A* **87**, 042309 (2013).
- [18] I. Almog, Y. Sagi, G. Gordon, G. Bensky, G. Kurizki and N. Davidson, *J. Phys. B* **44**, 154006 (2011).
- [19] G. A. Álvarez, and D. Suter, *Phys. Rev. Lett.* **107**, 230501 (2011).
- [20] M. G. A. Paris, *arXiv:1401.4194v2*.
- [21] C. Benedetti, F. Buscemi, P. Bordone, M. G. A. Paris, *Phys. Rev. A* **89**, 032114 (2014).
- [22] Ł. Cywiński, *arXiv:1308.3102v1*.
- [23] C. W. Helstrom, *Quantum Detection and Estimation Theory* (Academic Press, New York, 1976).
- [24] J. D. Malley, J. Hornstein, *Statist. Sci.* **8**, 433 (1993).
- [25] S. Braunstein, C. Caves, *Phys. Rev. Lett.* **72**, 3439 (1994).

- [26] D. C. Brody, L. P. Hughston, Proc. Roy. Soc. Lond. A **454**, 2445 (1998); A **455**, 1683 (1999).
- [27] M. G. A. Paris, Int. J. Quant. Inf. **7**, 125 (2009).
- [28] B. M. Escher, L. Davidovich, N. Zagury, R. L. de Matos Filho, Phys. Rev. Lett. **109**, 190404 (2012); B. M. Escher, R. L. de Matos Filho, and L. Davidovich, Braz. J. Phys. **41**, 229 (2011).
- [29] C. Benedetti, A.P. Shurupov, M.G. A. Paris, G. Brida, and M. Genovese, Phys. Rev. A **87**, 052136 (2013).
- [30] R. Blandino, M. G. Genoni, J. Etesse, M. Barbieri, M. G. A. Paris, P. Grangier, and R. Tualle-Broui, Phys. Rev. Lett **109**, 180402 (2012).
- [31] A. Monras, Phys. Rev. A **73**, 033821 (2006).
- [32] L. Pezzé, A. Smerzi, G. Khoury, J. F. Hodelin, and D. Bouwmeester, Phys. Rev. Lett. **99**, 223602 (2007).
- [33] S. Olivares and M. G. A. Paris, J. Phys. B **42**, 055506 (2009).
- [34] B. Teklu, S. Olivares and M. G. A. Paris, J. Phys. B **42**, 035502 (2009).
- [35] M. Kacprowicz, R. Demkowicz-Dobrzanski, W. Wasilewski, K. Banaszek, I. A. Walmsley, Nature Phot. **4**, 357 (2010).
- [36] H. Cable, G. A. Durkin, Phys. Rev. Lett. **105**, 013603 (2010).
- [37] G. A. Durkin, New J. Phys. **12** 023010 (2010).
- [38] M. G. Genoni, S. Olivares, M. G. A. Paris, Phys. Rev. Lett. **106**, 153603 (2011); M. G. Genoni, S. Olivares, D. Brivio, S. Cialdi, D. Cipriani, A. Santamato, S. Vezzoli, M. G. A. Paris, Phys. Rev. A **85**, 043817 (2012).
- [39] N. Spagnolo, C. Vitelli, V. G. Lucivero, V. Giovannetti, L. Maccone, and F. Sciarrino, Phys. Rev. Lett. **108**, 233602 (2012).
- [40] T. Rocheleau, T. Ndukum, C. Macklin, J. B. Hertzberg, A. A. Clerk, and K. C. Schwab, Nature **463**, 7275 (2010).
- [41] A. D. O'Connell, M. Hofheinz, M. Ansmann, R. C. Bialczak, M. Lenander, E. Lucero, M. Neeley, D. Sank, H. Wang, M. Weidesl, J. Wenner, J. M. Martinis, A. N. Cleland, Nature **464**, 697 (2010).
- [42] M. Brunelli, S. Olivares, M. G. A. Paris, Phys. Rev. A **84**, 032105 (2011).
- [43] M. Brunelli, S. Olivares, M. Paternostro, M. G. A. Paris, Phys. Rev. A **86**, 012125 (2012).
- [44] G. De Chiara and M. Palma, Phys. Rev. Lett. **91**, 090404 (2003).
- [45] J.-W. Mao, J.-X. Chen, W.-H. Huang, B.-Q. Li, W.-K. Ge, Phys. Rev. E **81**, 031123 (2010).
- [46] A. Fiasconaro and B. Spagnolo, Phys. Rev. E **80**, 041110 (2009).
- [47] C. Benedetti, M. G. A. Paris, Int. J. Quantum. Inf. **12**, 1461004 (2014).
- [48] N. Wiener, Proc. London Math. Soc. **22**, 454 (1924).
- [49] H. S. Wio, *Path Integrals for Stochastic Processes* (World Scientific, Singapore, 2013).
- [50] E. L. Lehman, G. Casella, *Theory of Point Estimation*, (Springer, Berlin, 1998).